Take it personal! Genetic differences in G protein-coupled receptors as studied with label-free technology

Hillger, J.M.

CHAPTER 6

Personal lymphoblastoid cell lines reveal E354Q polymorphism effects on GIP receptor signaling

Julia M. Hillger

Maartje J. Sprietsma

Jaqueline S. Gerritsen

Zi Wang

Thea Mulder-Krieger

Dorret I. Boomsma

P. Eline Slagboom

Adriaan P. IJzerman

Laura H. Heitman

Manuscript in preparation

Abstract

The glucose-dependent insulinotropic polypeptide receptor (GIPR) is a G protein-coupled receptor that plays an important role in whole-body metabolism. One missense Single Nucleotide Polymorphism (SNP) rs1800437 coding for amino acid change E354Q in the GIPR, has been associated with several diseases including diabetes and the risk of bone fractures. We investigated the functional effects of this SNP in personal cell lines from a panel of individuals with different genotypes for the polymorphism. Genotype effects were measured using a sensitive *in vitro* assay, i.e. a label-free cell morphology-based assay (xCELLigence), in combination with personal lymphoblastoid cell lines (LCLs) derived from Netherlands Twin Register participants. Responses to the endogenous agonist GIP showed enhanced potency in *Q354* homozygous individuals, while heterozygotes showed mixed effects. A mutational study of the E354 residue in recombinant HEK293 cells expressing GIPR did not show differences in potency, but revealed a reduced duration of effect for *Q354*, which was not observed in LCLs. Taken together, this study provides more insight into E354Q-related physiological changes as they occur in the human individual, and thereby contributes to precision medicine for GIPR-related pathologies.

Introduction

The glucose-dependent insulinotropic polypeptide receptor (GIPR) is a class B G protein-coupled receptor (GPCR) which is part of the glucagon receptor family [1]. It plays an important role in whole-body metabolism, such as glucose homeostasis and particularly insulin secretion, lipid uptake and bone density [2-4]. In the emerging era of precision medicine, it is becoming apparent that genetic differences between individuals can affect both drug action and susceptibility to disease. Several of such examples for GPCR polymorphisms already exist [5-8]. For the GIPR, previous research has linked Single Nucleotide Polymorphisms (SNPs) to various pathological conditions including obesity and diabetes [9-12]. One SNP of particular interest is rs1800437, which is a missense SNP that changes a glutamic acid to a glutamine at amino acid 354 of the receptor (E354Q). This E354Q is the only frequent one of 227 known GIPR missense variants that occurs in more than 1% of the population, namely with a Minor Allele Frequency (MAF) of 16% [13, 14]. Interestingly, several studies have associated this SNP with insulin resistance, type II diabetes, cardiovascular disease and the risk of bone fractures [3, 12, 15, 16]. Furthermore, a number of functional studies have indicated roles for this polymorphism in for instance receptor (in)activation [17] and desensitization [3].

This polymorphism could therefore play an important role in disease susceptibility of, as well as influence drug treatment. Mapping and understanding the effects of this polymorphism not only in the overall population, but in the individual patient is therefore paramount [18]. However, the E354Q polymorphism has so far been the subject of either cohort or candidate gene studies, or of functional studies in which its effect was analyzed in mouse cell lines or recombinant cell systems with artificially introduced mutations [3, 12, 15, 16, 19]. Despite their merits such cellular systems are further away from the physiological condition in humans. To better understand the influence of polymorphisms on receptor response in an individual, an ideal set-up would therefore be to use patient-derived material as a model system.

One example of such are lymphoblastoid cell lines (LCLs), which are commonly used to store a person's genetic material, as is done by many large scale genetic consortia such as the International HapMap and 1000 genomes projects [20-24]. We recently published a methodology that allows measurement of GPCR function in such LCLs, with which we were able to detect the effect of polymorphisms in two other GPCRs, the adenosine A_{2A} receptor and cannabinoid receptor 2 (**Chapter 4, 5**). Responses were measured using the xCELLigence,

a newly developed, highly sensitive label-free cellular assay technology. This assay measures changes in cell morphology in real-time as opposed to techniques traditionally employed in GPCR research such as ligand binding or second messenger accumulation assays, which use static, one-molecule-detection [25-28].

In the current study we have applied this real-time morphological assay to assess effects of the GIPR polymorphism E354Q in LCLs. We characterized GIPR responses in a selection of individuals from the Netherlands Twin Register (NTR) [29]. Subsequently, we performed an E354 mutational study in HEK293 cells using the same cellular assay technology as a functional read-out to provide a direct comparison to the effects observed in the LCLs.

Material and methods

Chemicals and reagents

Fibronectin from bovine plasma, ATP, unsupplemented Roswell Park Memorial Institute (RPMI) 1640 cell culture medium (25 mM HEPES and $NaHCO_3$) and Dulbecco's Modified Eagles Medium – high glucose (DMEM) were purchased from Sigma Aldrich (Zwijndrecht, The Netherlands). Fetal calf serum (FCS) was obtained from Thermo Fisher Scientific (Breda, The Netherlands). GIP was purchased from Tebu-Bio (Heerhugowaard, The Netherlands), while (Pro^3)GIP was obtained from American Peptide Company Inc (Sunnyvale, CA, USA). All other chemicals and reagents were of analytical grade and obtained from commercial sources, unless stated otherwise.

Lymphoblastoid cell line generation

For all 78 individuals of the Netherlands Twin Register (NTR, VU, Amsterdam, NL) [29] included in this study, lymphoblastoid cell lines (LCLs) were generated in accordance with previous Chapters (eg. **Chapter 3**) by the Rutgers Institute (Department of Genetics, Piscataway, NJ, USA). Briefly, peripheral B-lymphocytes were transformed with Epstein-Barr Virus (EBV) using a standard transformation protocol [29] and subsequently cryopreserved.

Cell culture

LCLs were cultured as suspension cells in RPMI 1640 (25 mM HEPES and $NaHCO_3$) supplemented with 15% FCS, 50 mg/mL streptomycin, 50 IU/mL penicillin, at 37°C in a humidified 5% CO_2 incubator, as described previously (**Chapter 3**). Cells were subcultured twice a week at a ratio of 1:5 on 10 cm ø plates and disposed after maximally 120 days.

HEK293 cells were grown in culture medium consisting of DMEM supplemented with

10% FCS, 50 mg/mL streptomycin and 50 IU/mL penicillin at 37°C in a humidified 7% CO_2 incubator. Cells were subcultured twice a week at a ratio of 1:10 to 1:30 on 10 cm ø plates.

DNA constructs and mutant generation

cDNA encoding the human GIPR (ORF: NM_000164) with an N-terminal FLAG-tag cloned into the pcDNA3.1(+) vector was purchased from GenScript (Hong Kong, China). Primers to generate the E354Q mutant were designed using the online QuickChange Primer Design tool [30] and produced by Eurogentec (Maastricht, The Netherlands). Primer sequences were forward: GCTGGGTGTCCACCAGGTGGTGTTTGC, and reverse: GCAAACACCACCTGGTGGACACCCAGC (5'–3'). The GIPR mutant was generated based on the QuikChange site-directed mutagenesis method (Agilent Technologies, La Jolla, CA, USA) [31] using pfu polymerase (Promega, Madison, WI, USA) in an 18-cycle mutagenic PCR. Subsequently, template DNA was digested by *DpnI* (New England Biolabs, Ipswich, MA, USA) treatment. PCR products were transformed into chemically competent DH5α cells (Life Technologies, Carlsbad, CA, USA) and purified using a standard Qiagen Miniprep kit (QIAGEN Benelux B.V., Venlo, The Netherlands). DNA concentration and purity were determined by NanoDrop 2000 (Thermo Fisher Scientific) and mutations were confirmed through double stranded DNA sequencing by the Leiden Genome Technology Center (LUMC, Leiden, The Netherlands).

HEK293 transfection

hGIPR constructs were transiently transfected into HEK293 cells. HEK293 cells were cultured in supplemented DMEM as stipulated above as a monolayer on 10-cm ø culture plates to 80–90% confluency. Transfections were performed using Lipofectamine 2000 (Thermo Fisher Scientific) and 8 µg of plasmid per 10-cm ø culture plate, in accordance with the manufacturer's instructions. As per these instructions, both plasmid and lipofectamine were diluted in unsupplemented OptiMEM (Thermo Fisher Scientific), subsequently mixed and incubated for 20 min at room temperature. Medium of HEK293 cells was exchanged to unsupplemented OptiMEM, after which the plasmid-lipofectamine mixture was deposited on the cells. After 6 hours of incubation with this mixture, cells were used for experiments.

Label-free whole-cell analysis (xCELLigence RTCA system)

Instrumentation principle

Cellular assays using the xCELLigence RTCA system [25] were performed in accordance with

previously published protocols (**Chapter 3, 4**) [32]. The detection principle of this real-time cell analyzer (RTCA) is based on electrical impedance. Gold electrodes are embedded on the bottom of the microelectronic E-plates. When cells attach to these, they alter the local ionic environment at the electrode-solution interface, thereby generating impedance. Relative changes in impedance (Z) are recorded in real-time and summarized in the dimensionless parameter Cell Index (CI). The CI at any given time point is defined as $(Z_i\text{-}Z_0)$ Ω /15 Ω, where Z_i is the impedance at each individual time point. Z_0 is defined as 0, as it represents the baseline impedance in the absence of cells. The resulting time-resolved impedance profile directly reflects any changes in degree of adhesion, cell number, viability and morphology, which are also the typical cellular parameters that are affected by GPCR signaling [25, 26].

General protocol

Prior to any experiment, background impedance (Z_0) was measured after adding 45 µL, or in case of antagonist experiments 40 µL, of the respective culture media to the E-plate wells. Subsequently, cells were harvested, centrifuged at 200g for 5min and resuspended in their corresponding fresh medium. xCELLigence assays on LCLs were performed as described previously (**Chapter 3**) with some minor modifications. Briefly, LCLs were harvested and seeded onto fibronectin-coated glass-bottom E-plates (50 µg/ml) at 100,000 cells/well. Transiently transfected HEK293 cells were harvested 4-6 hours following transfection by trypsinization, spun down once and seeded onto uncoated PET E-plates at 80,000 cells/well. Cell counts were performed with Trypan blue staining on a BioRad TC10 automated cell counter. After cell seeding, E-plates were clicked in the xCELLigence recording station in an incubator (37°C, 5% CO_2). Impedance was measured overnight for 18 hours, after which the cells were stimulated with a GPCR agonist or vehicle control in (5 µl), unless specified otherwise. For GIP concentration-response curves in LCLs, ATP [100 µM] was taken along to provide a receptor-independent reference of response height. As GIP and (Pro^3)GIP were stored as aliquots in Phosphate Buffered Saline (PBS), as per vendor instructions, PBS was used as vehicle control. The final PBS concentration upon ligand or vehicle addition was kept constant at 0.5 % PBS for all wells and assays. Agonist concentration-response curves were generated by stimulating cells with increasing concentrations of GIP. For the (Pro^3)GIP assay, cells were pre-incubated for 30 minutes with 5 µl of vehicle control or a high concentration of (Pro^3)GIP [1 µM]. Subsequently, cells were challenged with vehicle control or a submaximal agonist concentration of GIP corresponding to its EC_{80} value (concentration causing 80% of maximal effect) of *E354* and *Q354*, respectively (31.6 nM and 3.16 nM). All compound responses were recorded for at least 3 hours following agonist or vehicle addition.

ELISA

HEK293 cells were transiently transfected with the hGIPR E354, Q354 variant or mock as described above. Flat-bottom sterile 96 wells plates were coated with 50 µl poly-D-lysine (20 mg/L) (Sigma Aldrich) for 10 minutes. Cells were harvested, counted and seeded at 80,000 cells/well as described under the xCELLigence protocol, and medium was exchanged to normal culture medium. Cells were grown overnight at 37°C and 7% CO_2. Twenty-four hours post transfection, cells were washed once with PBS, fixed with 3,7% formaldehyde for 10 minutes and incubated in Tris-buffered saline (TBS) with 2% bovine serum albumin (BSA) for 30 minutes at room temperature. Cells were then incubated with 1:1000 anti-Q1-FLAG monoclonal antibody (Sigma Aldrich) and 1:1250 goat-anti-mouse HRP conjugated IgG antibody (Thermo Fisher Scientific) subsequently. Immunoreactivity was visualized by addition of 3,3',5,5'-tetramethylbenzidine (Sigma Aldrich). After 5 minutes the reaction was stopped by addition of 0.2M H_2SO_4. Absorbance was measured at 450 nm using a Victor plate reader (Perkin Elmer, Groningen, The Netherlands).

qPCR

qPCR on LCLs was performed as described previously (**Chapter 5**). Briefly, for each cell line RNA of three independent samples was isolated with RNeasy Plus Mini (QIAGEN, Venlo, the Netherlands). cDNA was randomly primed from 500 ng of total RNA using ReverstAid H Minus First Strand cDNA synthesis Kit (ThermoFisher, Breda, The Netherlands). The primers for GIPR were CGTCTGCTGGGACTATGCTG forward and TCTCCAAAGTCCCCATTGGC reverse. Household gene β-actin was used as internal control to enable comparison between individuals, and the primers for this were ATTGCCGACAGGATGCAGAA forward and GCTGATCCACATCTGCTGGAA reverse. Real-time qPCR was performed in triplicate for each sample using SYBR Green PCR (Applied Biosystems, part of ThermoFisher) on a 7500 Real-Time PCR System (Applied Biosystems). qPCR data were collected and analyzed using SDS2.3 software (Applied Biosystems). The $2^{-\Delta\Delta Ct}$ method was used to express relative mRNA amounts after correction for β-actin control mRNA.

Data analysis

xCELLigence

xCELLigence data were analyzed as described previously (**Chapter 3**). Experimental data were captured with RTCA Software 1.2 (ACEA, San Diego, CA, USA). Ligand responses were normalized to the last time point prior to compound addition resulting in a Normalized Cell Index (NCI). For HEK293, this was done directly in the RTCA program, while for the LCLs the

NCI was calculated in GraphPad Prism as the small (and sometimes negative) growth curves of LCLs hindered this calculation in the RTCA program. The NCI corrects for non-receptor-related variations that could for instance arise from a slight difference in seeding density, individual differences in proliferation rate and well-plate 'edge effects'. Data were exported to GraphPad Prism 6.0 (GraphPad Software Inc., San Diego, CA, USA) for further analysis. The lowest concentration of GIP was subtracted as baseline to correct for ligand-independent effects. Responses after compound addition were analyzed using AUC within 30 minutes for GIP and 60 minutes for ATP in LCLs, and 4 hours for GIP in HEK293hGIPR, due to the differences in duration of response. For analysis of the duration of response in HEK293hGIPR, responses were defined as highest NCI (Max NCI) observed at specific time points after compound addition. Peak values, AUC and experimental ΔCI or NCI traces were used for construction of bar graphs or concentration–effect curves by nonlinear regression and calculation of EC_{50} (concentration causing half maximal effect) and EC_{80} (concentration causing 80% of maximal effect) values. E_{max} (maximum effect) values of compounds were derived from maximal responses within the analyzed timeframe. All E_{max} values were normalized to the *E354* variant (individual E4 for LCLs).

Statistics

All values obtained are means of at least three independent experiments performed in duplicate on the same cell line, unless stated otherwise. When comparing multiple means or multiple instances of two means, statistical significance was calculated using a one-way analysis of variance (ANOVA) with Fisher's least significant difference (LSD) test, for example comparison of multiple pEC_{50} values for LCLs or percentage of response at certain time points for HEK293 cells. Comparison of two values was done with Student's t-test, for instance pEC_{50} values of HEK293 cells.

Processing of SNPs and genetic data

As described in previous Chapter 4, the SNP data of the individuals included in the current study were obtained from the Genomes of the Netherlands consortium (GoNL, *http://www.nlgenome.nl/*) [33], in which the NTR takes part. The SNP data were analyzed in-house using PLINK, an open-source whole genome association analysis toolset [34, 35]. For the current study, SNPs within the boundaries of the *GIPR* gene (Ensembl gene: ENSG00000010310) as defined by the human genome overview GRCh37 (*http://grch37.ensembl.org/index.html*) were extracted. Subsequently, SNPs were annotated

according to position (e.g. coding sequence, exon) and SNP type (e.g. missense) based on GRCh37 and dbSNP (*http://www.ncbi.nlm.nih.gov/SNP/*).

Results

Genotypes and NTR study

To study the effect of GIPR polymorphisms using LCLs of the NTR, we first determined the GIPR genotypes in the NTR population. This constituted a selection of in total related and unrelated 78 individuals of the NTR for whom both genetic information and corresponding LCLs were available. **Table 1** provides an overview of the SNPs present in the GIPR gene of this NTR population. We found a total of 23 SNPs with varying location, type and frequency. None were rare as all occurred in more than 10% of this NTR population, but two SNPs were extremely frequent as they were found in more than 40% of the NTR individuals (i.e. SNPs no. 22 and 23, rs9749225 and rs2238689, respectively). Of note, frequencies of most SNPs within this population were similar to the global MAF, with some exceptions that were found more frequently (e.g. SNP 22, rs9749225) or less frequently (e.g. SNP no. 14, rs35568293). Most commonly, SNPs were located within introns, with the exception of three. Two of those were located in other non-coding regions, namely the 3'-UTR. Finally, there was only one missense variant, rs1800437, which is in fact the polymorphism causing E354Q by changing a codon from GAG to CAG. Approximately 21% of the NTR individuals carried the minor allele of this SNP (i.e. CAG), which therefore provided sufficient individuals to perform a study on the effect of this polymorphism.

The preference for any genetic study is to include multiple unrelated individuals of each genotype, and if possible of both genders. Here, we also used the unique family set-up of the NTR for selecting individuals for inclusion into our study. The individuals from NTR included in GoNL comprised of trio's, with two genetically unrelated individuals, the parents, and an offspring. In a small number of families, two children, which were monozygotic or dizygotic twins, were included. As summarized in **Table 2**, we selected individuals to include: 1) one family with two monozygotic twins (family 1), whose comparability of response is a basic requirement to allow any conclusions from the experiments presented here in association with genotype; 2) one family in which the parents were opposing homozygotes and their offspring thus a heterozygote (family 2), where this special genetic relationship allowed further conclusions on genotype-related effects, and 3) three additional individuals to be able to study several unrelated individuals of each genotype. Of note, the maximum number

Table 1. SNPs found in GIPR gene in NTR individuals. Publicly annotated SNPs according to the dbSNP (*http://www.ncbi.nlm.nih.gov/SNP/)* within the *GIPR* gene in the selected NTR population, ordered based on increasing frequency in the NTR. Locations and gene boundaries were as defined by human genome overview GRCh37 (gene boundaries 19: 46171502 – 19:46186982). Type and global MAF are from the respective dbSNP pages (*http://www.ncbi.nlm.nih.gov/SNP/*).

Nr	SNP	Location	Minor Allele	Major Allele	Minor Allele count (NTR)	Type (dbSNP)	Global MAF (dbSNP)
1	rs11671664	19:46172278	A	G	0.114	Intron variant	A=0.1552
2	rs34089191	19:46176723	C	G	0.114	Intron variant, upstream variant 2KB	C=0.2171
3	rs55669001	19:46177235	C	T	0.114	Intron variant, upstream variant 2KB	C=0.1528
4	rs58304657	19:46176405	C	G	0.114	Intron variant, upstream variant 2KB	C=0.2192
5	rs9749185	19:46175416	A	G	0.114	Intron variant	A=0.1534
6	rs61373376	19:46183586	T	C	0.1579	Intron variant	T=0.0887
7	rs10423928	19:46182304	A	T	0.2105	Intron variant	A=0.1719
8	rs11672660	19:46180184	T	C	0.2105	Intron variant, upstream variant 2KB	T=0.1595
9	rs1800437	19:46181392	C	G	0.2105	Downstream variant 500B, missense, nc transcript variant	C=0.1611
10	rs2238690	19:46178886	A	G	0.2105	Intron variant, upstream variant 2KB	A=0.2512
11	rs2238691	19:46179043	A	G	0.2105	Intron variant, upstream variant 2KB	A=0.1603
12	rs2302382	19:46172569	A	C	0.2105	Intron variant	A=0.1627
13	rs34783010	19:46180414	T	G	0.2105	Intron variant	T=0.1595
14	rs35568293	19:46179110	C	T	0.2105	Intron variant, upstream variant 2KB	C=0.3155
15	rs7250736	19:46184012	G	C	0.2105	Intron variant	G=0.2514
16	rs7250754	19:46184061	A	C	0.2105	Intron variant	A=0.2514
17	rs2334255	19:46186150	T	G	0.2193	Downstream variant 500B, utr variant 3 prime	T=0.2606
18	rs12709891	19:46185217	A	C	0.2281	Nc transcript variant, utr variant 3 prime	A=0.2602
19	rs10404234	19:46183476	G	C	0.2368	Intron variant	G=0.2103
20	rs4803846	19:46180150	A	G	0.2368	Intron variant, upstream variant 2KB	A=0.2119
21	rs2878163	19:46183954	G	T	0.2456	Intron variant	G=0.2103
22	rs9749225	19:46175445	A	T	0.4035	Intron variant	T=0.2145
23	rs2238689	19:46178661	C	T	0.4211	Intron variant, downstream variant 500B, upstream variant 2KB	C=0.4880

Nc = non-coding; utr = untranslated region

Table 2. Selected set of NTR individuals studied for the E354Q GIPR polymorphism.

Identity				E354Q	
Group	Individual	Gender	Code	Genotype	Amino acid
Family 1	Father 1	Male	E1	GG	E
	Mother 1	Female	E2	GG	E
	Twin 1A	Female	E3	GG	E
	Twin 1B	Female	E4	GG	E
Family 2	Father 2	Male	E5	GG	E
	Mother 2	Female	Q1	CC	Q
	Twin 2A	Male	EQ1	CG	E/Q
Additional	Additional 1	Female	EQ2	CG	E/Q
	Additional 2	Female	EQ3	CG	E/Q
	Additional 3	Male	Q2	CC	Q

of *Q354* individuals was investigated, as only two of such were available in the NTR population. Moreover, both genders were represented in each group. Thus in total, we studied responses of LCLs of 10 individuals (**Table 2**).

GIPR signaling can be measured sensitively in LCLs using xCELLigence

To confirm the suitability of LCLs for studying GIPR effects, we first performed an initial qPCR as well as a response screen on the xCELLigence. The qPCR on a set of *E354* and *Q354* homozygous individuals revealed that mRNA of the GIPR was present in all individuals (**Fig. 1F**). mRNA levels were not consequently linked to genotype as significant differences were observed between individuals both with the same or different genotypes, and even between monozygotic twins E3 and E4.

Subsequently, we assessed GIPR responses on the xCELLigence in comparison with responses to ATP. The latter was used as a reference ligand as it is known to target GPCRs that are highly expressed and activation of these leads to cellular responses in LCLs (**Chapter 3**) [36, 37]. In **Fig. 1A** an exemplary experiment on the LCLs is presented, where cellular growth and responses were recorded in real-time. LCL seeding resulted in an initial increase in impedance related to cell adhesion, growth and division. Subsequent addition of a GPCR agonist such as ATP or GIP induced an immediate increase of impedance to a peak level of similar height, which gradually decreased towards a plateau. However, the duration

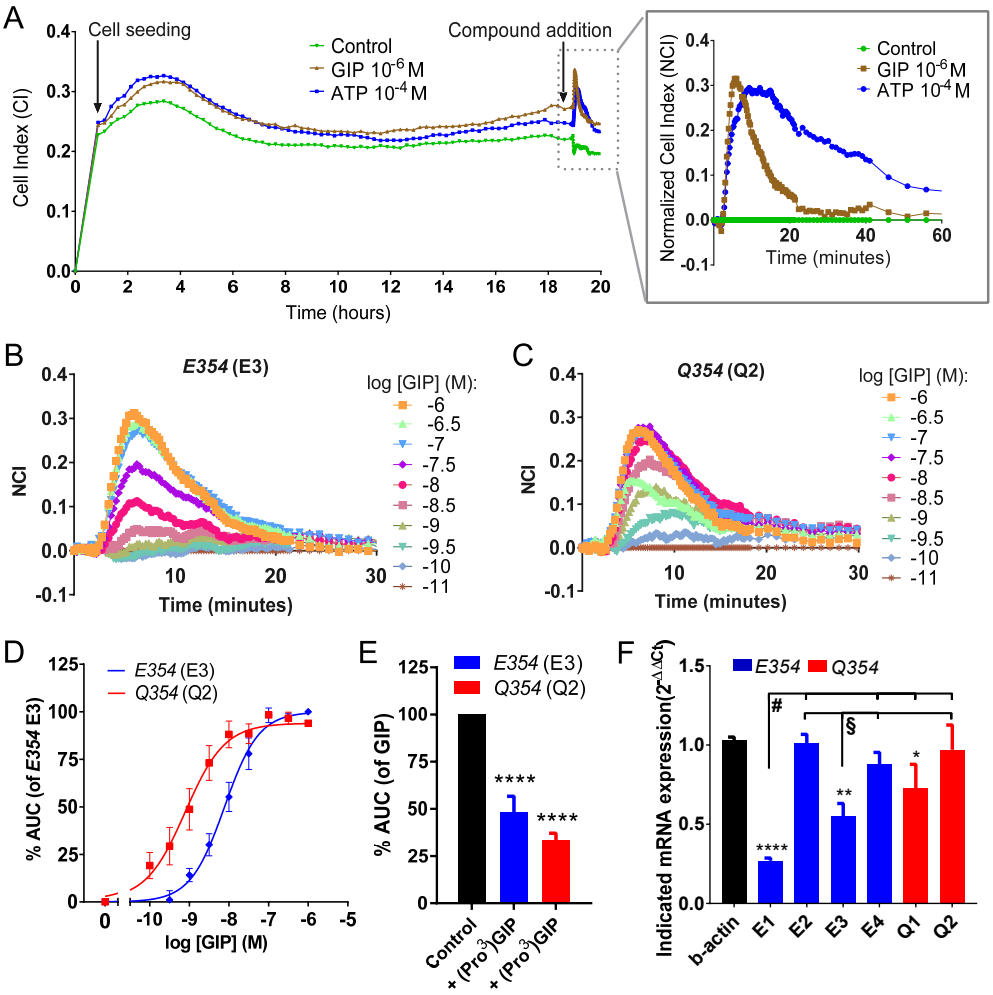

Figure 1. Characterization of GIPR response in LCLs with varying E354Q genotypes. (**A**) Representative example of a full real-time impedance plot and baseline-corrected responses of LCLs from one individual (E3) to GIP [1 µM] and ATP [100 µM]. Representative examples of baseline-corrected real-time impedance plot for one *E354* (E3, **B**) and one *Q354* (Q2, **C**) homozygous individual as a function of different concentrations of the endogenous agonist GIP ranging from 1 µM to 10 pM. (**D**) GIP concentration-response curves derived from AUC of NCI within 30 minutes after agonist addition, normalized to *E354* (E3). pEC_{50} and E_{max} values are summarized in *Table 3*. (**E**) Inhibitory effect of (Pro^3)GIP [1 µM] on response to a submaximal dose of GIP ([3.16 nM] for *Q354* and [31.6 nM] for *E354*). (**F**) Results of real-time qPCR show mRNA expression of GIPR in 6 selected individuals with *E354* or *Q354* genotype. Statistic differences were determined by one-way ANOVA with Fisher's LSD test. *p≤0.05, **p≤0.01, ***p≤0.001, ****p≤0.0001. For **F**, differences to β-actin are indicated with asterisk. Expression differences between individuals were # = E1 **** to E2, *** to E4 and Q2, ** to Q1. § = E3 ** to E2 and Q2, * to E4. In figures **A**, **B** and **C**, representative traces are shown. In figures **D**, **E** and **F** means ± SEM of three or more separate experiments performed in duplicate (**D** and **E**) or triplicate (**F**) are shown.

of response caused by ATP or GIP differed. For GIP, the response returned to baseline levels within a period of 30 minutes, where ATP induced cellular changes lasting over 60 minutes. This showed that LCL responses to GPCR agonists are receptor specific with regard to shape and duration as measured using the xCELLigence technology.

Finally, we tested inhibition of GIP signaling effects in LCLs using the only commercially available GIPR selective antagonist, (Pro^3)GIP, which did not elicit a response on its own upon addition to the LCLs (**Supplemental Fig. S1**). As shown in **Fig. 1E**, (Pro^3)GIP was able to (partly) diminish GIP responses.

Together, these results show that GIPR signaling in LCLs can be measured sensitively and specifically using the xCELLigence methodology.

E534Q alters endogenous agonist potency of GIPR in personal cell lines

Subsequently, LCL responses of the selection of E354Q individuals by the endogenous agonist GIP were determined. The resulting concentration-effect curves are summarized in **Fig. 1B-D**. GIP efficacy and potency values for the entire set of 10 individuals are summarized in **Table 3**. Responses between the monozygotic twins E3 and E4 were highly comparable, confirming that the LCLs are a suitable model system to study genetic effects on the GIPR.

Shown in **Fig. 1B and 1C** are representative examples of the real-time baseline-corrected responses of two unrelated individuals representing the two possible E354Q homozygous genotypes, i.e. one *E354* and one *Q354* homozygous individual, respectively. Irrespective of genotype, these LCLs showed similar responses to GIP which did not differ significantly in overall shape or duration. However, differences in GIP effects were observed, especially in potency as can be seen in **Fig. 1D** where the concentration-response curves of these two individuals are given. Furthermore, both *E354* and *Q354* homozygous individuals showed highly similar effects in potency within their respective group of individuals with the same genotype, but these groups differed significantly from each other. Specifically, pEC_{50} values of GIP on *E354* individuals ranged from 7.90 ± 0.07 (E4) to 8.34 ± 0.08 (E2), while the same values on LCLs of *Q354* individuals were 8.96 ± 0.25 (Q1) and 9.12 ± 0.08 (Q2). Therefore, GIP potency was significantly higher (i.e. 4-17-fold) in LCLs from *Q354* homozygous individuals (Q1 and Q2), as opposed to the *E354* homozygotes. Interestingly, the LCLs of heterozygotes showed mixed effects, as their potency values showed a large spread with a range of 7.91 ± 0.11 (EQ2) to 9.32 ± 0.14 (EQ1). Heterozygotes thus also differed significantly from each other by 4- to 26-fold, which was similar to the difference between *Q354* and *E354* homozygous individuals. In general, heterozygotes were closer in potency to *Q354*

Table 3. Endogenous agonist GIP potency and efficacy per individual's LCL.. Data represent means ± SEM for three or more different experiments performed in duplicate. E_{max} was corrected for growth curve height by NCI and normalized to the individual with the highest response. Statistically significant differences between individuals were determined by one-way ANOVA with Fisher's LSD post-hoc test. Significant differences are highlighted by blue = to *E354* individuals, red = to *Q354* individuals and green = to E354Q heterozygotes. Individual p-values are given in *Supplemental table S1*.

Group	Individual	pEC_{50} ± SEM	pEC_{50} Significantly different	E_{max} ± SEM	E_{max} Significantly different
Family 1	E1	8.14 ± 0.07	to all Q; to all E/Q except EQ2	87.3 ± 25.6	to all Q; to EQ2, E2, E3
	E2	8.34 ± 0.08	to all Q; to all E/Q; to E4	26.6 ± 7.1	to E1, E4, E5; to all E/Q except EQ2
	E3	8.11 ± 0.05	to all Q; to all E/Q except EQ2	43.5 ± 4.0	to E1, E4
	E4	7.90 ± 0.07	to all Q; to all E/Q except EQ2; to E2	100.0 ± 22.6	to all Q; to EQ2, E2, E3
	E5	8.14 ± 0.12	to all Q; to all E/Q except EQ2	79.8 ± 11.3	to all Q; to EQ2, E2
Family 2	Q1	8.96 ± 0.25	to all E; to all E/Q except EQ3	17.2 ± 7.3	to E1, E4, E5; to all E/Q except EQ2
Additional	EQ1	9.32 ± 0.14	to all E; to all E/Q; to Q1	76.7 ± 14.5	to E2, EQ2, Q1
	EQ2	7.91 ± 0.11	to all Q; to all E/Q; to E2	33.2 ± 4.2	to all E/Q; to E1, E4, E5
	EQ3	8.73 ± 0.08	to all E; to all E/Q; to Q2	74.7 ± 11.1	to all Q; to EQ2, E2
	Q2	9.12 ± 0.08	to all E; to all E/Q except EQ1	40.9 ± 5.5	to E1, E4, E5, EQ3

(EQ1, EQ3) than to *E354* individuals (EQ2 only). This was irrespective of gender, and not smaller between related family members. In fact, in family 2 who encompassed a *E354* father and *Q354* mother, GIP potency in LCLs of their child was not in between the two but instead much closer to *Q354*.

Besides potency, we also assessed GIP efficacy for which we did not observe a genotype-related trend, despite a wide range of efficacies with many significant differences (**Table 3**). The individuals with the highest efficacy were three *E354* homozygotes, followed by two heterozygotes. Both *Q354* individuals showed lower efficacy, with Q1 the lowest of all. The trend was however not consistent, as other *E354* homozygotes such as E2 showed efficacies lower than some *Q354*. Furthermore, the monozygotic twin pair E3 and E4 differed largely in efficacy. Thus, GIP efficacies were not consistent with genotype. Of note, GIP efficacy was not related to gender either, as for instance for *E354* the individuals with highest and lowest efficacy were both female. Finally, there was also no clear relationship to GIPR mRNA levels, as for example the two cell lines with the highest E_{max}, E4 and E1, differed greatly in their mRNA levels (**Fig. 1F**).

In conclusion, the responses of the NTR individuals' LCLs revealed that the E354Q polymorphism increased the potency of endogenous agonist GIP in *Q354* homozygotes, while heterozygotes showed mixed effects with respect to GIP potency. The efficacy of GIP was not affected by this polymorphism.

Mutational study E354 in HEK293 cells shows differences in duration of effect

To provide a more direct comparison to our personal cell lines, we performed a mutational study using transiently transfected HEK293 cells and measured their responses upon GIP addition using the xCELLigence. An example of the real-time readout of cellular growth and responses to GIP for HEK293 cells transiently transfected with mock, *E354* and *Q354* is presented in **Fig. 2A**. Addition of GIP to mock-transfected HEK293 cells did not induce significant changes in impedance, while it resulted in an immediate effect in *E354* or *Q354* transfected cells. In both cases, impedance increased to a peak level within 120 minutes and subsequently declined towards baseline, which it did not reach though, even after 240 minutes. Thus, the GIP response dynamics of HEK293hGIPR cells are different from LCLs, especially in response duration.

Fig. 2B and **2C** display examples of the respective real-time traces of *E354* and *Q354* HEK293hGIPR cells responses to GIP from which concentration-effect curves were constructed by analyzing the AUC over 4 hours of response (**Fig. 2D**). The overall effect of GIP in this time period did not differ significantly between *E354* and *Q354* with respect to potency

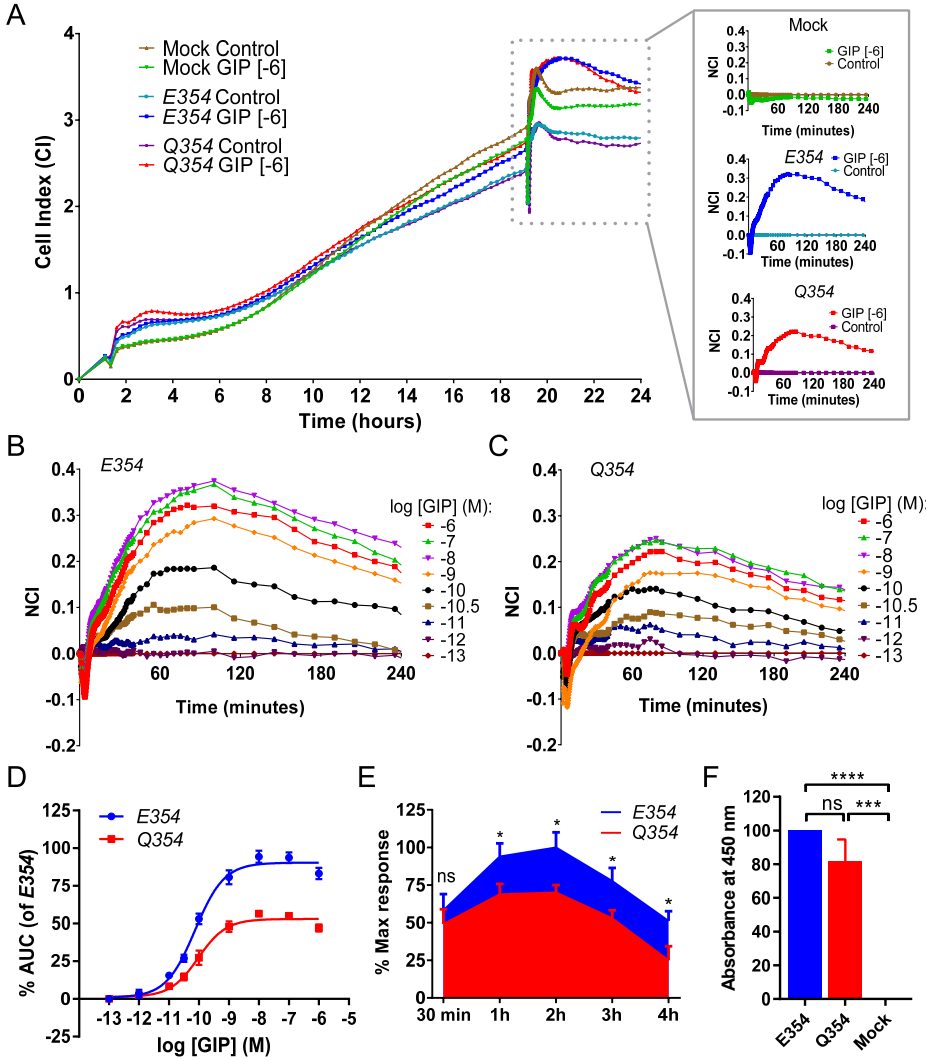

Figure 2. Characterization for hGIPR response in HEK293 cells transiently transfected with *E354* or *Q354* variant. Representative example of a full real-time impedance plot and baseline-corrected responses of mock, *E354* and *Q354* transiently transfected HEK293 cells (**A**) and real-time baseline-corrected concentration-responses curves for (**B**) *E354* and (**C**) *Q354* transfected HEK293 cells. (**D**) Concentration-response curves derived of AUC from NCI within 4 hours after GIP addition for *E354* and *Q354* transfected HEK293 cells. pEC_{50} values were 10.25 ± 0.06 and 10.18 ± 0.08, while E_{max} values were 100 ± 2.9 % and 56.9 ± 6.4 %, respectively. Potency was not significantly different, while E_{max} differed by **** as determined by Student's t-test. (**E**) Percentage highest baseline-corrected response to GIP [1 µM] of *Q354* versus *E354* at several time points. The overall highest response of *E354* was set to 100%. (**F**) Cell-surface expression of *E354* and *Q354* over mock transfected HEK293 cells as determined by FLAG-tag ELISA, which was not significantly different between the two variants. All data are presented as means ± SEM of three or more separate experiments performed in duplicate. Statistic differences were determined by two-way (**E**) or one-way (**F**) ANOVA with Fisher's LSD test. *p≤0.05, **p≤0.01, ***p≤0.001, ****p≤0.0001.

(pEC_{50} of 10.25 ± 0.06 and 10.18 ± 0.08, respectively). Efficacy, however, defined as the maximally achieved overall AUC, was significantly altered (E_{max} of 100 ± 2.9 % and 56.9 ± 6.4 %, respectively). Thus, the overall cellular effect through *Q354* was lower than through *E354*, which was mostly due to how the height of the cellular effect diverged over time (**Fig. 2E**). Specifically, at 30 minutes after agonist addition *E354* and *Q354* showed virtually the same height of response to GIP, while the effect on *Q354* declined towards baseline more rapidly after that time. At 4 hours after GIP addition, the effect on *Q354* was only 49 % of *E354*.
Finally, we confirmed that any differences between *E354* and *Q354* receptor variants transiently transfected in HEK293 cells were not due to differences in cell surface expression by performing ELISA (**Fig. 2F**). In conclusion, the mutational study of E354Q in transiently transfected HEK293 cells showed no differences in potency. In contrast, significant differences were found in efficacy as the height as well as duration of response were decreased in *Q354*.

Discussion

Genetic differences between individuals can affect both drug action and susceptibility to diseases, as is increasingly recognized under the concept of personalized or precision medicine [38]. The GIPR missense SNP E354Q has been associated with diseases including diabetes and bone-fracture risk [12, 15, 16] and shown to have functional effects in mouse cell lines or recombinant cell systems [3, 16, 19]. However, results from such animal and recombinant cells may not be directly translatable to the human individual. Additionally, several of these studies yielded conflicting results. To provide a better link with the physiological situation we studied the effect of this SNP in personal cell lines, i.e. LCLs of a set of individuals from the NTR [29].

The E354Q was present in 21% of NTR individuals, which was in accordance with its global MAF [14]. Most of the other SNPs in the *GIPR* gene (**Table 1**) were located in introns, as is common for intron-containing GPCRs due to the evolutionary conservation of the different regions [39, 40]. Thus for functional studies in LCLs, we selected 10 individuals including two or more unrelated individuals of both genders for each of the three E354Q genotypes (**Table 2**). The set of monozygotic twins used as control for genotype-unrelated effects [29, 41] showed highly comparable responses to the endogenous agonist GIP (**Fig. 1, Table 3**), confirming LCLs are a suitable model system. Remarkably, E354Q affected GIP potency consistently over all individuals, while being independent on gender and family-relation. GIP had higher potency in all *Q354* versus *E354* homozygotes, while heterozygotes

showed a wide spread in potency, differing between each other and from both homozygotes (**Fig. 1, Table 3**). Interestingly, precisely this heterozygous variant but not the homozygous *Q354* has been associated with cardiovascular disease [15]. Conversely, only *Q354* homozygotes were associated with reduced serum C-peptide concentrations, a parameter related to insulin levels [16]. Finally, Torekov *et al.* found minor allele carriers had lowered bone mineral density, but only *Q354* homozygotes had increased risk for certain fractures [12]. The effect of E354Q heterozygosity is therefore not straightforward, and could vary depending on disease. Thus, investigating heterozygosity is imperative for deciphering E354Q pharmacology.

In our study, the E354Q SNP showed clear (genotype-related) effects in LCLs of NTR individuals, mainly on the potency of the endogenous ligand GIP. For instance, GIP potency was highly comparable in the monozygous twins E3 and E4 (**Table 3**). In contrast, the efficacy was not genotype-related (**Table 3**), as for example the same monozygous twins E3 and E4 differed greatly in their E_{max}. Efficacy was also not related to other characteristics such as gender (**Table 2**, **Table 3**) or GIPR mRNA levels (**Fig. 1F**). For example, E4 and E1 were the two cell lines with the highest E_{max}. Contrarily, E4 had high GIPR mRNA levels while E1 exhibited the lowest of all individuals. It has to be kept in mind that mRNA expression levels do not necessarily correlate with functional protein expression on the cellular membrane, a feature well-known in literature [42, 43]. Thus, it appears that neither differences in mRNA levels or E_{max} reveal any E354Q-related effects on functional GIPR expression. Notably, the maximal effects of both GIP and another ligand which targets a completely different set of GPCRs, namely ATP, showed a similar ranking of individuals (*data not shown*). Hence it is possible that the differences in maximal effects reflect each individual's overall cell properties such as viability, proliferation rate and adherence to electrodes, which are not specifically GPCR-related but are known to affect xCELLigence readout [25-28].

Overall, the E354Q SNP showed outspoken effects in LCLs of NTR individuals. It has been suggested that E354, based on functionality of the same $E^{6.48}$ in other class B GPCRs, has a potentially important role in ligand binding and receptor (in)activation [17]. It was shown that mutation to an alanine caused a loss of hydrogen bonding network interactions, resulting in a constitutively active mutant with higher GIP affinity and potency, but unchanged efficacy [17]. Mutation to glutamine may have similar effects by reducing interaction strength, thus causing increased potency yet similar efficacy for agonists, which is in accordance with the observations in LCLs. However, several studies examining functional effects of E354Q in mouse cell lines or recombinant cell systems yielded conflicting results. For instance, Fortin *et al.* noted that *Q354* reduced induction of cAMP production in

recombinant HEK293 cells, while neither Almind *et al.* nor Mohammad *et al.* found any effect on cAMP formation in CHO cells or mouse adipocytes, respectively [3, 16, 19]. A similar discrepancy was observed for antagonism of GIPR in LCLs, which is considered a potential treatment for GIPR-related metabolic abnormalities such as diabetes [44]. When we tested (Pro^3)GIP, the only commercially available GPR antagonist, in LCLs, it partly inhibited GIP activation (**Fig. 1E**) in correspondence to its reported low potency [45]. Interestingly, in our hands (Pro^3)GIP merely acted as an antagonist (**Supplemental Fig. S1**), while Sparre-Ulrich *et al*. reported it to be a full or partial agonist [46]. It stands to notice that the above findings were established in recombinant or non-human cell systems. On the other hand, LCLs are a completely human system that endogenously expresses hGIPR. Lastly, all of these observations were obtained using typical endpoint or second messenger assays, which focus on one part of a cellular response only. Systems such as the xCELLigence offer the advantage of measuring whole-cell responses in real-time as opposed to a static, one-molecule-detection [25-28]. Hence, such label-free whole-cell assays are preferable over typical endpoint assays to minimize bias [47].

To further investigate the influence of the model system used, we measured E354Q mutational effects in a common recombinant system, namely transiently transfected HEK293 cells, using the exact same xCELLigence assay to provide direct comparison. As in LCLs, *E354* and *Q354* were not differentially expressed and we observed a receptor-specific impedance signal (**Fig. 2A, F**). Interestingly, HEK293hGIPR cells showed a response duration vastly different from LCLs (30 minutes for LCLs versus over 240 minutes for HEK293hGIPR). In addition, overall GIP potency was at least 5-fold higher than in LCLs. However, previously published potencies also span a wide range, even within the same cell type. GIP potencies on transiently transfected HEK293hGIPR cells expressing *E354* range from 0.9 pM [19] to 490 ± 30 pM [17], and even 3.63 nM on CHO cells [16], all of which values that were determined in cAMP-based assays.

Besides differences in GIP effects in general, E354Q specifically showed divergent pharmacological effects in HEK293hGIPR and LCLs. Specifically, E354Q did not affect potency in HEK293hGIPR, but had a significant influence on efficacy in terms of height and duration of cellular effects, which were both lower for *Q354* than for *E354* (**Fig. 2**). This is in accordance with findings by Mohammad *et al*. in the same cell type, who established that *Q354* slowed receptor recycling to the cell surface following agonist stimulation [3]. This could lead to a decreased availability of receptors to mediate the cellular effects as measured by the xCELLigence, thus lower and declining more rapidly over time.

It is well-established that the behavior of GPCRs is dependent on the cellular context [48, 49]. HEK293 cells are a prototypical recombinant system prone to receptor overexpression, whereas LCLs are personal cell lines with endogenous levels of receptor expression. This emphasizes the importance of using primary or derived (i.e. endogenous immortalized) human cell systems that offer more physiological relevance to confirm any effects established in other cell systems.

Irrespective of the model system, it is essential to consider findings in the light of physiological and pathological conditions. Consumption of meals induces GIP blood concentrations to approx. 100 pM, which return to previous levels around 20 pM within 3 to 4 h [3, 50-52]. It is clear that such physiological concentrations of GIP cannot reach a maximal effect in *E354* LCLs, where potencies are around 10 nM (Table 3). However, GIP potency on *Q534* LCLs was higher and in the pM range. This makes potency differences extremely relevant for physiological effects, as receptors with increased potency such as the *Q354* variant could mediate a larger response. If this variant additionally shows a shorter effect duration or slower recycling to the surface after GIP stimulation, as pointed at by our results and those of Mohammad *et al.* in HEK293 cells [3], the combination could contribute to lowered GIP sensitivity and, for instance, increasing the risk of insulin resistance. Replicating these findings in cell types directly involved in the physiological functions of GIP, such as adipocytes from patients versus healthy volunteers containing both E354Q GIPR forms, could offer more conclusive results.

In conclusion, our study with personal cell lines that endogenously express E354Q shows that this polymorphism has a strong effect on receptor response, namely by increasing GIP potency, which can affect the physiological function of the receptor. Furthermore, a mutational study in recombinant HEK293 cells revealed a reduced effect duration for *Q354*, which was not observed in LCLs. Thus, the effects of E354Q differ depending on the model system used. By studying E354Q effects in personal cell lines, we aimed to increase the link with the real-life situation and to provide more insight into physiological changes as they occur in the human individual, and thereby contribute to precision medicine for GIPR-related pathologies.

Data Access

The LCLs used in this study were kindly provided within the framework of this collaboration [29] and are part of the Netherlands Twin Register (NTR; *http://www.tweelingenregister.org/en/*), and part of the Center for Collaborative Genomic

Studies on Mental Disorders (NIMH EQ34 MH068457-06). Data and biomaterials (such as cell lines) are available to qualified investigators, and may be accessed by following a set of instructions stipulated on the National Institute of Mental Health (NIMH) website (*https://www.nimhgenetics.org/access_data_biomaterial.php*).

Acknowledgements

We thank Dr. A. Brooks (Department of Genetics, Rutgers University, Piscataway, NJ, USA) for preparation of the lymphoblastoid cell lines. The research presented in this manuscript was supported by the Center for Collaborative Genomic Studies on Mental Disorders (NIMH EQ34 MH068457-06). Funding for the GoNL was provided by the Netherlands Organization for Scientific Research (184021007) to BBMRI-NL. The NTR acknowledges support from the Netherlands Organization for Scientific Research (grant NWO 480-15-001/674: Netherlands Twin Registry Repository: researching the interplay between genome and environment).

References

1. Usdin, T.B., et al., *Gastric inhibitory polypeptide receptor, a member of the secretin-vasoactive intestinal peptide receptor family, is widely distributed in peripheral organs and the brain.* Endocrinology, 1993. **133**(6): p. 2861-70.
2. Irwin, N. and P.R. Flatt, *Therapeutic potential for GIP receptor agonists and antagonists.* Best Pract Res Clin Endocrinol Metab, 2009. **23**(4): p. 499-512.
3. Mohammad, S., et al., *A naturally occurring GIP receptor variant undergoes enhanced agonist-induced desensitization, which impairs GIP control of adipose insulin sensitivity.* Mol Cell Biol, 2014. **34**(19): p. 3618-29.
4. Holst, J.J., et al., *Searching for the physiological role of glucose-dependent insulinotropic polypeptide.* J Diabetes Investig, 2016. **7 Suppl 1**: p. 8-12.
5. Davies, M.A., et al., *Pharmacologic analysis of non-synonymous coding h5-HT2A SNPs reveals alterations in atypical antipsychotic and agonist efficacies.* Pharmacogenomics J, 2006. **6**(1): p. 42-51.
6. Docherty, S.J., et al., *A genetic association study of DNA methylation levels in the DRD4 gene region finds associations with nearby SNPs.* Behav Brain Funct, 2012. **8**: p. 31-44.
7. Ishiguro, H., et al., *Brain cannabinoid CB2 receptor in schizophrenia.* Biol Psychiatry, 2010. **67**(10): p. 974-82.
8. Sadee, W., et al., *Genetic variations in human G protein-coupled receptors: implications for drug therapy.* AAPS pharmSci, 2001. **3**(3): p. 54-80.
9. Sauber, J., et al., *Association of variants in gastric inhibitory polypeptide receptor gene with impaired glucose homeostasis in obese children and adolescents from Berlin.* Eur J Endocrinol, 2010. **163**(2): p. 259-64.
10. Vogel, C.I., et al., *Gastric inhibitory polypeptide receptor: association analyses for obesity of several polymorphisms in large study groups.* BMC Med Genet, 2009. **10**: p. 19.
11. Saxena, R., et al., *Genetic variation in GIPR influences the glucose and insulin responses to an oral glucose challenge.* Nat Genet, 2010. **42**(2): p. 142-8.
12. Torekov, S.S., et al., *A functional amino acid substitution in the glucose-dependent insulinotropic polypeptide receptor (GIPR) gene is associated with lower bone mineral density and increased fracture risk.* J Clin Endocrinol Metab, 2014. **99**(4): p. E729-33.
13. NCBI. *GIPR, http://www.ncbi.nlm.nih.gov/gene/2696, Accessed 21.07.2016*. 2016 03.07.2016 21.07.2016].
14. dbSNP. *http://www.ncbi.nlm.nih.gov/projects/SNP/snp_ref.cgi?rs=1800437 ; Accessed 21.07.2016*. 2016 21.07.2016].
15. Nitz, I., et al., *Association analyses of GIP and GIPR polymorphisms with traits of the metabolic syndrome.* Mol Nutr Food Res, 2007. **51**(8): p. 1046-52.
16. Almind, K., et al., *Discovery of amino acid variants in the human glucose-dependent insulinotropic polypeptide (GIP) receptor: the impact on the pancreatic beta cell responses and functional expression studies in Chinese hamster fibroblast cells.* Diabetologia, 1998. **41**(10): p. 1194-8.
17. Cordomi, A., et al., *Functional elements of the gastric inhibitory polypeptide receptor: Comparison between secretin- and rhodopsin-like G protein-coupled receptors.* Biochem Pharmacol, 2015. **96**(3): p. 237-46.

18. Venkatakrishnan, A.J., et al., *Molecular signatures of G-protein-coupled receptors.* Nature, 2013. **494**(7436): p. 185-94.
19. Fortin, J.P., et al., *Pharmacological characterization of human incretin receptor missense variants.* J Pharmacol Exp Ther, 2010. **332**(1): p. 274-80.
20. Sie, L., S. Loong, and E.K. Tan, *Utility of lymphoblastoid cell lines.* J Neurosci Res, 2009. **87**(9): p. 1953-9.
21. Sugimoto, M., et al., *Steps involved in immortalization and tumorigenesis in human B-lymphoblastoid cell lines transformed by Epstein-Barr virus.* Cancer research, 2004. **64**(10): p. 3361-4.
22. Abecasis, G.R., et al., *A map of human genome variation from population-scale sequencing.* Nature, 2010. **467**(7319): p. 1061-73.
23. Welsh, M., et al., *Pharmacogenomic discovery using cell-based models.* Pharmacological reviews, 2009. **61**(4): p. 413-29.
24. Wheeler, H.E. and M.E. Dolan, *Lymphoblastoid cell lines in pharmacogenomic discovery and clinical translation.* Pharmacogenomics, 2012. **13**(1): p. 55-70.
25. Yu, N., et al., *Real-time monitoring of morphological changes in living cells by electronic cell sensor arrays: an approach to study G protein-coupled receptors.* Anal Chem, 2006. **78**(1): p. 35-43.
26. Fang, Y., *Label-Free Receptor Assays.* Drug Discov Today Technol, 2011. **7**(1): p. e5-e11.
27. Rocheville, M., et al., *Mining the potential of label-free biosensors for seven-transmembrane receptor drug discovery.* Progress in molecular biology and translational science, 2013. **115**: p. 123-42.
28. Fredholm, B.B., et al., *International Union of Basic and Clinical Pharmacology. LXXXI. Nomenclature and classification of adenosine receptors--an update.* Pharmacol Rev, 2011. **63**(1): p. 1-34.
29. Willemsen, G., et al., *The Netherlands Twin Register biobank: a resource for genetic epidemiological studies.* Twin Res Hum Genet, 2010. **13**(3): p. 231-45.
30. Program, Q.P.D. *http://www.genomics.agilent.com/primerDesignProgram.jsp?toggle=uploadNow&mutate=true&_requestid=1185053*. [cited 2015 November 3].
31. Liu, H. and J.H. Naismith, *An efficient one-step site-directed deletion, insertion, single and multiple-site plasmid mutagenesis protocol.* BMC Biotechnol, 2008. **8**: p. 91.
32. Guo, D., et al., *Functional efficacy of adenosine A(2)A receptor agonists is positively correlated to their receptor residence time.* British journal of pharmacology, 2012. **166**(6): p. 1846-59.
33. *Whole-genome sequence variation, population structure and demographic history of the Dutch population.* Nature genetics, 2014. **46**(8): p. 818-25.
34. Purcell, S., et al., *PLINK: a tool set for whole-genome association and population-based linkage analyses.* Am J Hum Genet, 2007. **81**(3): p. 559-75.
35. Purcell, S., *PLINK v1.07, http://pngu.mgh.harvard.edu/purcell/plink/*.
36. Jacob, F., et al., *Purinergic signaling in inflammatory cells: P2 receptor expression, functional effects, and modulation of inflammatory responses.* Purinergic signalling, 2013. **9**(3): p. 285-306.

37. Lee, D.H., et al., *Expression of P2 receptors in human B cells and Epstein-Barr virus-transformed lymphoblastoid cell lines.* BMC immunology, 2006. **7**: p. 22-33.
38. Lu, Y.F., et al., *Personalized medicine and human genetic diversity.* Cold Spring Harb Perspect Med, 2014. **4**(9).
39. Kruglyak, L. and D.A. Nickerson, *Variation is the spice of life.* Nature Genetics, 2001. **27**(3): p. 234-236.
40. Small, K.M., et al., *Gene and protein domain-specific patterns of genetic variability within the G-protein coupled receptor superfamily.* Am J Pharmacogenomics, 2003. **3**(1): p. 65-71.
41. Silventoinen, K., et al., *The CODATwins Project: The Cohort Description of Collaborative Project of Development of Anthropometrical Measures in Twins to Study Macro-Environmental Variation in Genetic and Environmental Effects on Anthropometric Traits.* Twin Res Hum Genet, 2015. **18**(4): p. 348-60.
42. Guo, Y., et al., *How is mRNA expression predictive for protein expression? A correlation study on human circulating monocytes.* Acta Biochim Biophys Sin (Shanghai), 2008. **40**(5): p. 426-36.
43. Vogel, C. and E.M. Marcotte, *Insights into the regulation of protein abundance from proteomic and transcriptomic analyses.* Nat Rev Genet, 2012. **13**(4): p. 227-32.
44. McClean, P.L., et al., *(Pro(3))GIP[mPEG]: novel, long-acting, mPEGylated antagonist of gastric inhibitory polypeptide for obesity-diabetes (diabesity) therapy.* British journal of pharmacology, 2008. **155**(5): p. 690-701.
45. Gault, V.A., et al., *Characterization of the cellular and metabolic effects of a novel enzyme-resistant antagonist of glucose-dependent insulinotropic polypeptide.* Biochemical and biophysical research communications, 2002. **290**(5): p. 1420-6.
46. Sparre-Ulrich, A.H., et al., *Species-specific action of (Pro3)GIP - a full agonist at human GIP receptors, but a partial agonist and competitive antagonist at rat and mouse GIP receptors.* British journal of pharmacology, 2016. **173**(1): p. 27-38.
47. Rocheville, M., et al., *Mining the potential of label-free biosensors for seven-transmembrane receptor drug discovery.* Oligomerization and Allosteric Modulation in G-Protein Coupled Receptors, 2012. **115**: p. 123.
48. Butcher, A.J., et al., *Differential G-protein-coupled receptor phosphorylation provides evidence for a signaling bar code.* J Biol Chem, 2011. **286**(13): p. 11506-18.
49. Tobin, A.B., A.J. Butcher, and K.C. Kong, *Location, location, location...site-specific GPCR phosphorylation offers a mechanism for cell-type-specific signalling.* Trends Pharmacol Sci, 2008. **29**(8): p. 413-20.
50. Jorde, R., et al., *Effect of gastrin on fasting and postprandial plasma GIP release in man.* Digestion, 1982. **25**(2): p. 81-7.
51. Lyssenko, V., et al., *Pleiotropic effects of GIP on islet function involve osteopontin.* Diabetes, 2011. **60**(9): p. 2424-33.
52. Tseng, C.C., et al., *Postprandial stimulation of insulin release by glucose-dependent insulinotropic polypeptide (GIP). Effect of a specific glucose-dependent insulinotropic polypeptide receptor antagonist in the rat.* J Clin Invest, 1996. **98**(11): p. 2440-5.

Supporting information

Supplemental Table S1. Significant differences in endogenous agonist GIP potency and efficacy per individual's LCL. Data represent pEC_{50} ± SEM and E_{max} ± SEM of at least three experiments performed in duplicate. Statistical analysis was performed by one-way ANOVA with Fisher's LSD post-hoc test. For pEC_{50}, a large difference between GG genotypes (*E354*) the CC genotype (*Q354*) compared to GG genotypes and a mixed effect for the heterozygote genotype. The E_{max} showed little differences that were not consistent with genotype. ns = not significant; *p≤0.05, **p≤0.01, ***p≤0.001, ****p≤0.0001.

Individuals	pEC_{50}		E_{max}	
	Summary	P Value	Summary	P Value
E1 vs. E2	ns	0.1670	**	0.0027
E1 vs. E3	ns	0.8819	*	0.0250
E1 vs. E4	ns	0.1156	ns	0.4986
E1 vs. E5	ns	0.9651	ns	0.7103
E1 vs. Q1	****	<0.0001	**	0.0015
E1 vs. EQ1	****	<0.0001	ns	0.6019
E1 vs. EQ2	ns	0.1278	**	0.0067
E1 vs. EQ3	***	0.0002	ns	0.4815
E1 vs. Q2	****	<0.0001	*	0.0103
E2 vs. E3	ns	0.1278	ns	0.3722
E2 vs. E4	**	0.0049	***	0.0004
E2 vs. E5	ns	0.2149	*	0.0128
E2 vs. Q1	***	0.0005	ns	0.6423
E2 vs. EQ1	****	<0.0001	*	0.0183
E2 vs. EQ2	**	0.0056	ns	0.7262
E2 vs. EQ3	*	0.0100	*	0.0105
E2 vs. Q2	****	<0.0001	ns	0.4081
E3 vs. E4	ns	0.1518	**	0.0048
E3 vs. E5	ns	0.8562	ns	0.0803
E3 vs. Q1	****	<0.0001	ns	0.2008
E3 vs. EQ1	****	<0.0001	ns	0.1078
E3 vs. EQ2	ns	0.1670	ns	0.5847
E3 vs. EQ3	***	0.0001	ns	0.0860
E3 vs. Q2	****	<0.0001	ns	0.8790
E4 vs. E5	ns	0.1330	ns	0.3210
E4 vs. Q1	****	<0.0001	***	0.0003
E4 vs. EQ1	****	<0.0001	ns	0.2546
E4 vs. EQ2	ns	0.9569	**	0.0011
E4 vs. EQ3	****	<0.0001	ns	0.1617
E4 vs. Q2	****	<0.0001	**	0.0015
E5 vs. Q1	****	<0,0001	**	0.0066
E5 vs. EQ1	****	<0.0001	ns	0.8877
E5 vs. EQ2	ns	0.1456	*	0.0272
E5 vs. EQ3	***	0.0006	ns	0.7947
E5 vs. Q2	****	<0.0001	*	0.0447
Q1 vs. EQ1	*	0.0406	**	0.0094

Q1 vs. EQ2	****	<0.0001	ns	0.4320
Q1 vs. EQ3	ns	0.1318	**	0.0054
Q1 vs. Q2	ns	0.2966	ns	0.2129
EQ1 vs. EQ2	****	<0.0001	*	0.0381
EQ1 vs. EQ3	***	0.0004	ns	0.9185
EQ1 vs. Q2	ns	0.1690	ns	0.0630
EQ2 vs. EQ3	****	<0.0001	*	0.0251
EQ2 vs. Q2	****	<0.0001	ns	0.6547
EQ3 vs. Q2	**	0.0041	*	0.0415

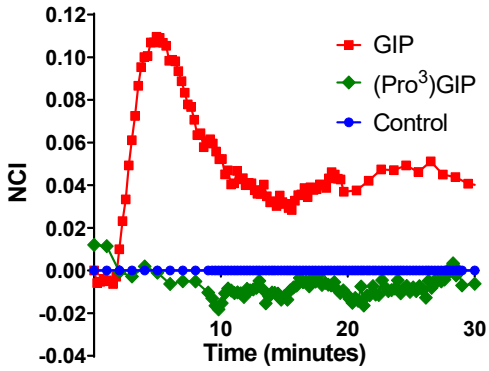

Supplemental Figure S1. (Pro^3)GIP response in LCLs. Representative example of a baseline-corrected responses to either (Pro^3)GIP [1 µM] or GIP [31.6nM] of LCLs from one *E354* individual, E3. Data is representative for three or more separate experiments performed in duplicate.